Received: 7 February 2021 | Revised: 12 May 2021 | Accepted: 14 May 2021

DOI: 10.1002/app.51180

ARTICLE

Applied Polymer SCIENCE WILEY

Electrochemical analyses of ZrO_2 dispersoid incorporated poly (styrene-methyl methacrylate) blend gel electrolytes for lithium-ion battery

Murugesan Ramachandran[1,2] | **Rengapillai Subadevi**[1] | **Palanisamy Rajkumar**[1] | **Rajendran Muthupradeepa**[1,3] | **Marimuthu Sivakumar**[1]

[1]Energy Materials Lab, Department of Physics, Science Block, Alagappa University, Tamil Nadu, India

[2]Department of Physics, Arumugam Pillai Seethai Ammal College, Tamil Nadu, India

[3]Department of Physics, Science and Humanities, Sree Sastha Institute of Engineering and Technology, Tamil Nadu, India

Correspondence
Marimuthu Sivakumar, #120, Energy Materials Lab, Department of Physics, Science Block, Alagappa University, Karaikudi-630003, Tamil Nadu, India.
Email: susiva73@yahoo.co.in, sivakumarm@alagappauniversity.ac.in

Funding information
Department of Science and Technology, Ministry of Science and Technology; Science and Engineering Research Board, Grant/Award Number: EMR/2016/006302; University Grants Commission, Grant/Award Number: 41-839/2012; Ministry of Human Resource Development, Grant/Award Number: F-24-51/2014

Abstract

Zirconium oxide (ZrO_2) filler is successfully synthesized with spherical morphology (particle size 170 nm) by co-precipitation technique earlier. The as-prepared ZrO_2 -(bare, 3, 6, 9, and 12 wt%) is spread into the augmented poly(styrene-co- methyl methacrylate) P(S-MMA)- poly vinylidene fluoride (PVdF) (25:75 of 27 wt%)-$LiClO_4$ (8 wt%)- ethylene carbonate and propylene carbonate (EC + PC) (1: 1 of 65 wt%) system. The solution casting technique is employed throughout the process. The structural, morphology, thermal and ionic conducting behavior of sample are examined. The highest conductivity is 1.2×10^{-2} S cm^{-1} at 303 K for P(S-MMA)-PVdF (25:75 of 27 wt%) $LiClO_4$ (8 wt%)- EC + PC (65 wt%) +6 wt% ZrO_2 system. The linear sweep voltammetry and the cyclic voltammetry tests are performed and the results are discussed. The optimized electrolyte is used to make the $LiFePO_4$/CGPE/Li confined 2032 coin cell couple. It holds the discharge capacity of 144 mAh g^{-1} at rate of 0.1 C with 88% coulombic efficiency.

KEYWORDS

batteries and fuel cells, composites, copolymers, nanoparticles, nanowires and nanocrystals, plasticizer

1 | INTRODUCTION

The utmost dynamic sources for human actions are energy. The cumulative energy demands cannot overcome by the present fossil fuels. Furthermore, the burning of fuel from the combustion engine pollutes the atmosphere, which causes the greenhouse effect. Many efforts have been taken to progress pollution-free, ecologically pleasant renewable resources to substitute the existing fuels. Secondary lithium-ion batteries (LIBs) are widely recognized due to their large working potential, huge energy density, lesser mass, extensive sequence life-cycle, eco-friendly, and so forth.[1–4] The complete cell performance of LIBs is determined by the basis of microstructure, electrical and electrochemical characteristics of the dynamic electrodes and electrolyte ingredients.

There are numerous constitutions in the battery, a transporting path material has been a significant one for LiBs, which precisely stimuli their electrochemical

performance. All present marketable LiBs comprising organic liquid electrolyte, owing to their high ionic conductivity at 303 K. Even though it exhibits security problem, owing to large gas evolution, small flashpoint, the creation of dendrites and outflow of electrolyte.[5,6] As a substitute, the solid polymer electrolyte (SPEs) is preferentially used to rectify the above-mentioned problems.[7]

There are many advantages of SPEs compared to the liquid electrolytes such as a simple strategy with chosen dimensions and outline, outflow resistant creation, struggle to shock and shaking, confrontation to compression and temperature differences, wide electrochemical constancy, good security, and so fourth. However, SPEs are also called dry polymer electrolytes. It does not keep any carbonate-based fluids, and the polymer host laterally with the Lithium salt performances as solid solvent. The ionic conductivity of (PEO-LiX) was found to be minimum at ambient temperature.[8] Improvisation of the conductivity of ions and stability of SPEs were made by the inclusion of plasticizer, polymer blend, and nanocrystalline ceramic filler into the polymer electrolytes (PEs).[9]

In general, high ionic conductivities (10^{-3} S cm^{-1}) at ambient temperature have been shown by gel polymer electrolytes (GPEs), but the tensile property has not been appropriate for commercial applications. Composite polymer electrolyte (CPE) has been formed with the addition of inorganic filler into the GPEs. The inorganic fillers such as TiO_2, SiO_2, ZrO_2, CeO_2, and Al_2O_3 serve as dense softeners, can critically obstruct the reorganization of the polymers chain, and it aids the dissociation of Li salts and also the movement of Lithium ions, owing to the Lewis acid–base contacts among the ceramic particles and electrolyte matrix or filler and charged species.[10–12] It intensely progresses grain morphology and electrochemical characteristics of electrolyte matrices.[13,14] Also, the physical and thermal properties of the electrolyte system can too be controlled by the choice and strategy of ceramic filler.

Among the studied nano-sized ceramic fillers, ZrO_2 is the better candidate to raise the conductivity of ions, because of its huge relative permittivity ($\varepsilon = 23$) and also large band gap.[15] The monoclinic ZrO_2 with spherical morphology with a particle size of 170 nm has been synthesized earlier by our group.[16] Uma et al.[17] described that the maximum conductivity obtained is 1.02×10^{-7} S cm^{-1} for a 10 wt% ZrO_2 based plasticizer polymer electrolyte system. Scrosati et al.[18] conveyed that the inclusion of inorganic filler into the polymer matrix, especially specific smaller size of particles and certain constitution, inhibit the structural behavior and indulge the unstructured segment, extremely leading assembly of the electrolyte matrix.

In GPEs, poly (vinylidene fluoride) (PVdF), Poly (methyl methacrylate) (PMMA), and polystyrene are generally utilized as host polymers because of their appealing properties. Among them, poly (styrene-methyl methacrylate) copolymer is identified as prompt material; the styrene unit can develop the tensile strength of GPE owing to its low attraction for the liquid electrolyte. PMMA acted as gelatinizing agent in the electrolyte with high anodic stability.[19] PVdF acts as a host polymer, which has high anodic stability owing to the strong electron diminishing efficient assembly (—C—F—). It has large relative permittivity ($\varepsilon = 8.4$) for an electrolyte matrix, it also aids in superior ionization of Lithium salts and therefore affords a higher gathering of charge transporters.[20]

Commonly, various methods are broadly used for the synthesis of solid/gel polymer or nanocomposite electrolyte, and so forth, Among these, solution casting has been easy to handle and an efficient matrix, namely, withdrawal of softener, phase inversion, hot press, solution casting, and electrospinning method to create the spongy electrolyte matrices with micron-size.[21–24]

To raise the conductivity of ions to the electrolyte matrices; the blending of polymers is a fashionable technique for making polymeric ingredients with greater characteristics, which has been inaccessible by unit component. The solution casting technique has been employed to synthesize the optimized ratio of the above parent ratio of polymer matrix- (bare, 3, 6, 9, and 12 wt%) of ZrO_2 polymer electrolyte. The as-synthesized samples had been analyzed by X-Ray diffraction (XRD), fourier Transform Infrared Spectroscopy (FTIR), field emission scanning electron microscope (FESEM), thermogravimetry/differential thermal analysis (TG/DTA), impedance studies. The optimized film has been performed Linear sweep voltammetry using SS/ZB3/Li cell. The optimized composition was used to fabricate the $LiFePO_4$/CGPE/Li-based 2032-coin cell. The cyclic voltammetry test and charge/discharge have been investigated.

2 | EXPERIMENTAL DETAILS

PVdF (mol wt 5.3×10^5) poly(styrene-co- methyl methacrylate) (P(S-MMA)) (mol wt 100–50) $LiClO_4$ (Aldrich), tetrahydrofuran (THF) had been utilized in the present work. The whole film had been synthesized using the solution casting method. The stoichiometric ratio of PVdF, P(styrene-methyl methacrylate), and $LiClO_4$ were taken and dried at 373 K, and then liquefy in extracted THF (E-Merck, Germany) PVdF was preheated at 60°C for 5 h and then included by the accumulation of plasticizers. The composition had been then agitated constantly till the assortment acquired a uniform gelatinous fluid.

The synthesized ZrO_2 (3, 6, 9, and 12 wt%) had been spread through the polymer matrices. The ensuing

mixture was dispensed onto a glass Petri plate and the THF was permissible to vanish at ambient room temperature. This process issued tensile steady and elastic films with width lies behind 50 and 100 μm. The electrolyte module was additionally dehydrated in a vacuum oven at a pressure of 10^{-3} Torr for 24 h at 333 K to eliminate any traces of THF. XRD analysis was accomplished to the electrolyte matrices at 303 K using an XPERT-PRO diffractometer with CuKα radiation. Functional group vibrations had been analyzed Fourier Transform Infrared analysis had been made using Thermo Nicolet 380 Instrument Corporation in the 4000–400 cm^{-1}. The scanning electron microscope (SEM, HITACHI-S 4800) had characterized the morphology of the sample. TG/DTA was measured on a thermal analyzer (SHI-MADZU DTA-60AH). The operation temperature was increased from 30 to 700°C under the N_2 atmosphere at a heat rate of 10°C min^{-1}.

Keithley (3300 LCZ meter) in the frequency between 40 and100 kHz had been used to measure the Conductivity of the electrolyte films. The as-prepared polymer matrices had been kept among a couple of stainless-steel terminals. They performed a hindering terminal to the ions. The linear sweep voltammetry (LSV) was performed using Stainless steel/ ZB3/Lithium cell. $LiFePO_4$/ZB3/Li half cell (CR 2032 type) is fabricated. Such that the cathode is prepared using the hybrid consisted of 80 wt% $LiFePO_4$ powder, 10 wt% carbon black, and 10 wt% PVdF were added together with N-methyl-2-pyrrolidone. The as-prepared cluster had been dispersed to Al- foil substrates and dehydrated at 373 K for 1 day under vacuum. Subsequently, the as-prepared foil had been cut to a 1×1 cm^2 size, the terminal had been arranged as cathode terminal Vs Lithium metal as counter and reference terminal in CR-2032 type coin-cells.[25] The LSV was performed using Stainless steel/ ZB3/Lithium cell. The LSV and CV tests were performed via BTS-55 Neware battery tester system between the potential 2 and 4.7 V and 2 and 4.3 V respectively at ambient temperature at a sweep rate of 1 mV s^{-1}.

3 | RESULT AND DISCUSSION

3.1 | XRD analysis

The XRD has inspected the crystalline nature of PVdF-P(S-MMA)-ZrO_2 polymer composites. Figure 1, illustrates the XRD patterns of raw PVdF, P(S-MMA), and pure $LiClO_4$, P(S-MMA) –PVdF- $LiClO_4$- EC + PC- ZrO_2 (bare, 3, 6, 9, and 12 wt%) which are named as ZB1, ZB2, ZB3, ZB4, and ZB5 respectively. The diffraction peaks that appear at $2\theta = 28.15$, 31.44, 34.13, and 57.15° are ascribed

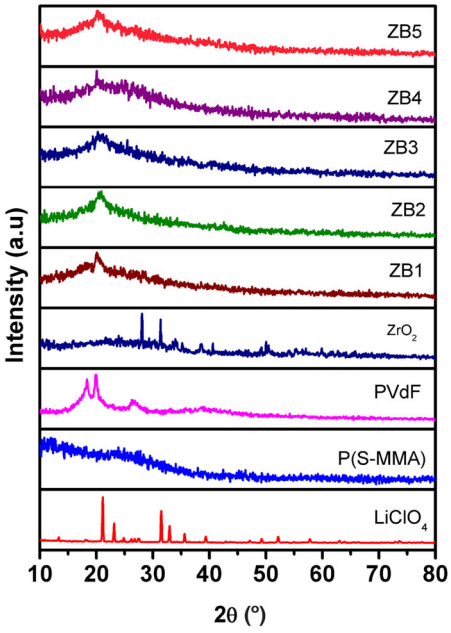

FIGURE 1 X-ray diffraction patterns of pure PVdF, P(S-MMA), $LiClO_4$, pure ZrO_2, bare P(S-MMA)-PVdF-$LiClO_4$-EC + PC-0 (ZB1), 3(ZB2), 6(ZB3), 9(ZB4), and 12 wt% (ZB5) of ZrO_2 based polymer electrolyte [Color figure can be viewed at wileyonlinelibrary.com]

to the monoclinic structure of ZrO_2 (JCPDS:89–9066). However, no peaks correspond to $LiClO_4$ have found in the diffraction patterns, owing to the formation of complexion between the polymer blend and Li salt. Figure 1 reveals that sample ZB3 possesses the lowest crystallinity (0.6%) among the systems studied. The peak relating to PVdF is diminished upon adding the ZrO_2 content up to 6 wt% and further increase of ZrO_2 causes the crystallinity due to the aggregation of ZrO_2 in the gel polymer blend electrolyte. The formation of amorphous nature has been revealed from the diffraction pattern of the complexes, which is responsible for the higher conductivity.[25–27]

3.2 | FTIR analysis

IR spectra of the as-prepared polymer matrices are shown in Figure 2. For all samples, OH stretching is observed in section 3600–3100 cm^{-1}. The CH_2 scissoring mode of MMA has appeared at 1480 cm^{-1}, it has been lifted to 1489 cm^{-1} in the complexes. The >C═O and > C═C < vibrational peaks of PVdF are appearing at 1630 and 1400 cm^{-1} respectively; these peaks are lifted to 1634 and 1398 cm^{-1} respectively in the matrices. This $\gamma_{C=O}$ skeletal breathing of EC appears at 1810 cm^{-1} is moved to the lower wavenumber in the electrolytes

which authorizes the EC are complexed into the electrolyte system.[28,29] The stretching vibration of Zr-O_2-Zr is appearing in 754 cm^{-1}, which is deviated in the complexes to 728 cm^{-1}. The absorption peaks of P(S-MMA) (626 and 1887 cm^{-1}), PVdF (1872,1560, 1072, and 509 cm^{-1}), $LiClO_4$ (553 and 2021 cm^{-1}), ZrO_2(418, 583, 1002, and 1556 cm^{-1}) are found, which have not appeared in the composite gel blend electrolyte systems. Furthermore, several new peaks are observed 1282, 1720, 2348, and 2934 cm^{-1} originate in the polymer complexes. The shifting of peaks, the vanishing of some peaks, and the addition of new points in the matrices concerning pure designate the complex creation in the polymer matrices.

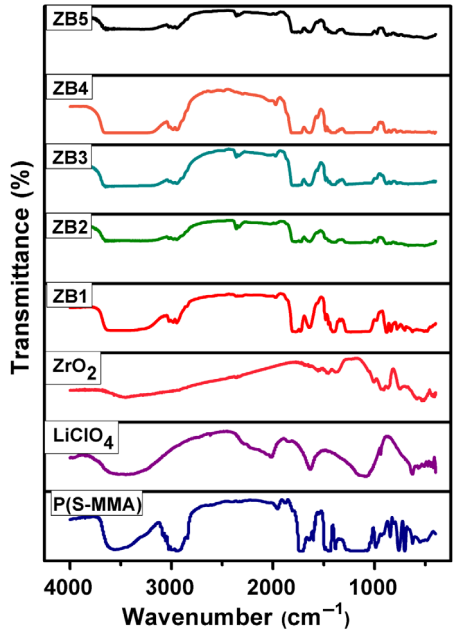

FIGURE 2 FTIR spectra of pure PVdF, P(S-MMA), $LiClO_4$, pure ZrO_2, bare P(S-MMA)-PVdF-$LiClO_4$-EC + PC(ZB1), 3 (ZB2), 6 (ZB3), 9(ZB4), and 12 wt% (ZB5) of ZrO_2 based polymer electrolyte [Color figure can be viewed at wileyonlinelibrary.com]

3.3 | AC impedance analysis

All the ac impedance measurements have been accomplished in the temperature range of 303–353 K using the atainless steel/ CPBE/stainless steel cell couple at a constant amplitude 5 mV and tabulated in Table 1. The ac impedance measurements have been performed for P(S-MMA)-PVdF (25:75 of 27 wt%)-$LiClO_4$(8 wt%)-EC: PC (1:1 of 65 wt%)- ZrO_2 (bare, 3, 6, 9 and 12) wt% electrolytes. The typical complex impedance plot of the 6 wt% of ZrO_2 based P(S-MMA)-PVdF(25:75 of 27 wt %)-$LiClO_4$(8 wt%)-EC: PC (1:1 of 65 wt%) system is shown in Figure 3(a). The x-intercept at the high-frequency region in the complex impedance plot provides the bulk resistance of the electrolytes, and the conductivity of ions is calculated by using the relation $\sigma = \frac{l}{R_b A}$ Here l, A, and R_b are thickness, area, and bulk resistance of the electrolyte system respectively. It has been observed from Table 1 that the electrolyte without the addition of filler exhibits the conductivity at 303 K is 0.3×10^{-3} S cm^{-1}, while incorporating the ZrO_2 filler with 3 wt%, conductivity enhances to one order of magnitude (1.3×10^{-3} S cm^{-1}) at 303 K. The ionic conductivity value rises upon the rise of ZrO_2 up to 6 wt% and further addition dips the conductivity down, which is very much visible from the complex impedance plot (Figure 3(a) inset). As increasing ZrO_2 content, the bulk resistance has shifted to the left and then shifted to the right, with minimum bulk resistance taken place at the composition 6 wt% of ZrO_2. From Table 1, it is implied that the maximum ionic conductivity is detected for the film ZB3 of 1.2×10^{-2} S cm^{-1} at 303 K. The value has been reasonably larger than that of the earlier report of Stephan et al.[30] for PVdF-co-HFP gel system and also higher than the report of Uma et al.[17] for PVC-$LiBF_4$-DBP-ZrO_2 system. The inclusion of inorganic particles improves free volume, which leads to larger salt detachment, and also the flaws presented during the spreading of ceramic fillers. A new transport mechanism ripens for the reason that of contact between polymer and inorganic particles. This transport

TABLE 1 Ionic conductivity values of P(S-MMA)-PVdF (25:75 of 27 wt%)-$LiClO_4$ (8 wt%)-EC:PC (1:1 of 65 wt%)- ZrO_2 (bare, 3, 6, 9, and 12) wt% (ZB1-ZB5) in the temperature range 303–343 K

Sample code	Ionic conductivity (S cm^{-1})						Activation energy (E_a) eV
	303 K	313 K	323 K	333 K	343 K	353 K	
ZB1	0.00031	0.00034	0.00046	0.00059	0.00063	0.00066	0.68
ZB2	0.0013	0.0025	0.0033	0.0044	0.0047	0.0052	0.39
ZB3	0.0119	0.0127	0.0152	0.0184	0.0259	0.031	0.23
ZB4	0.0071	0.0080	0.00906	0.00934	0.0098	0.014	0.29
ZB5	0.0047	0.0048	0.0051	0.0068	0.0070	0.0087	0.31

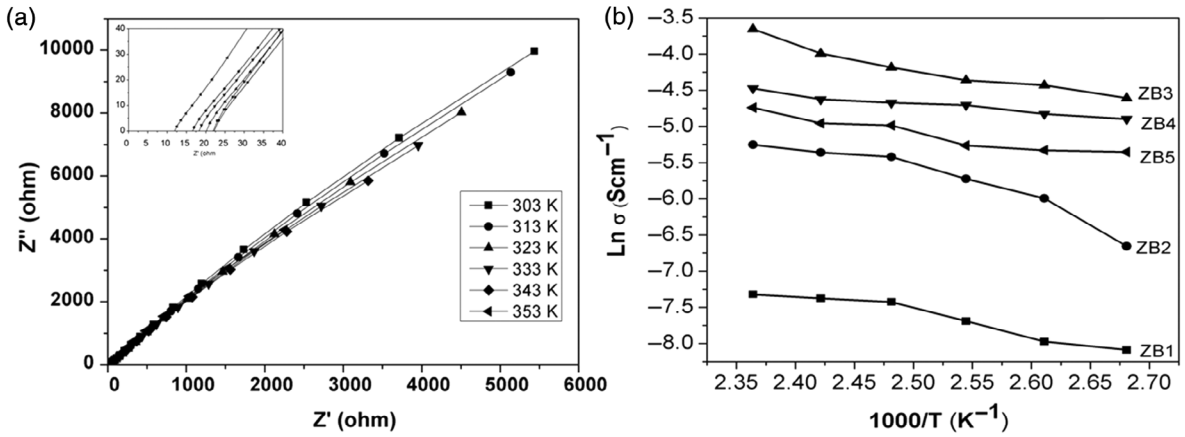

FIGURE 3 (a) Nyquist curve of P(S-MMA)-PVdF- $LiClO_4$-EC + PC +6 wt% ZrO_2 polymer electrolyte in the temperature range 303–353 K, (b) Arrhenius plots of P(S-MMA)-PVdF- $LiClO_4$ + EC + PC+ ZrO_2 (bare, 3, 6, 9, 12) wt% based electrolytes in the temperature range 303-353 K

mechanism is responsible for a track for the transmission of lithium ions.[31] Hence, rapid enrichment in the conduction of ions has been found for the hybrid polymer electrolyte. The enhancement in transporting phenomenon can also be recognized to the inorganic particles, substitute as nucleation cores for the creation of tiny structured and the inorganic phases assisting in the creation of unstructured stages in the polymer electrolyte. The 6 wt% ZrO_2 based complex (ZB3) has been attained the maximum conductivity. With further increase in ZrO_2 content, the conductivity value is declined down. Analogous observations had been previously obtained by Qian et al.[32] for PEO-based composite polymer electrolytes. This deed is a straight significance of large concentrations of ZrO_2, which indicates well-defined crystallite regions, and the ZrO_2 particles lean towards encumber ionic movement by acting as simple insulators. Also, this behavior is observed because the dispersed ceramics influenced the recrystallization kinetics of P(S-MMA) chains, thereby eventually stimulating localized amorphous regions and then the improvement of the Li^+ ion transport. Figure 3(b) shows the temperature-dependent ionic conductivity plots in the temperature range 303–353 K. The same trend was obtained for our previous studies on PVdF-PEMA based composite gel polymer electrolyte and PEO-based composite polymer electrolyte.[33,34] The whole complex, the conductivity rises with the rise of temperature and this can be updated by the free volume model. The arc of the plots shows that ionic conductivity appears to follow Vogel–Tammann–Fulcher relation,[35] which designates that transport of ions in polymer matrices requires polymer zig-zag motion. Miyamoto et al.[36] conveyed that the ionic conductivity improved with growing temperature as a consequence of the free volume model where, the temperature rises, the polymer electrolyte is enlarged simply and harvest free volume. Thus, solvated molecules, ions, or the polymer segments can conveyance into the free volume, affecting it to rise the movement of charge carriers. This improves the ions and polymer zig-zag motion that will, in turn, progress the ionic conductivity. The ionic conductivity of the prepared samples along with activation energy is depicted in Table 1. The activation energy of the system varies within the range 0.23–0.68 eV. We have calculated using Arrhenius equation $\sigma = \sigma_0 \exp(\frac{-E_a}{KT})$ Here σ–ionic conductivity of the sample, σ_0–pre exponential factor, E_a—activation energy, K–Boltzmann's constant, and T–absolute temperature. We plot the graph between 1000/T and log σ and take the slope of the curve (Figure 3(b)) hence we obtain the activation energy. It exposes that highly conducting film keeps smaller activation energy.

The huge conduction of ions and tensile durability of the electrolytes can be attained by filler (ZrO_2). Due to its high relative permittivity such as 89.6 at 40°C, the plasticizer EC provides the leading route for portable species. The addition of inorganic filler enhances the free volume, which accompanies larger salt separation, further the creation of imperfections because of an interaction of the polymer and the filler. Therefore, substantial enrichment in the conductivity is attained for the polymer system. The conductivity is ascribed to the fillers, acted as a seeding center for the creation of tiny structures, and the fillers aided in the creation of unstructured particles in the electrolyte matrices. Adding ZrO_2 in the electrolyte matrices affords the transporting pathways for the tiny species and increases the ion bouncing mechanism between the organizing spots and accompany by local structural relaxation and zig-zag mobility of the polymer. Also, the addition of plasticizers caused excellent pathways to ionic movement and provides more mobile charge

carriers by forming the networks.[37–39] Similarly, we compared with 265 nm ZrO_2 nano particles dispersed along the above polymer system. The results and discussion of the corresponding system has been provided in the Data S1 (Figure S1).

3.4 | SEM analysis

SEM is used to analyze the microstructure of the as-prepared samples. Figure 4(a–e) depicts SEM images of the prepared CGPE with the magnification of 1 K. As seen from Figure 4(a), the surface of P(S-MMA)-PVdF membrane without adding nano-ZrO_2, the pores exist due to the polymer matrix. During the increase of filler content up to 6 wt% the gelled electrolyte provides an excellent network formation (Figure 4(c)). Further inclusion of ceramic particles displays the accumulation of nanoparticles which has been shown in Figure 4(d,e). Such kind of accumulation obstructs the Lithium-ion with transport leads to a decline in conductivity. SEM pictures replicate the conductivity of ions quantities.[40]

3.5 | Thermal analysis

Thermogravimetric/differential temperature analysis is employed to recognize the thermal stability and decomposition of the polymers and their other constituents based on their volatility. Figure 5 depicts the TG/DTA curve for optimized parent polymer

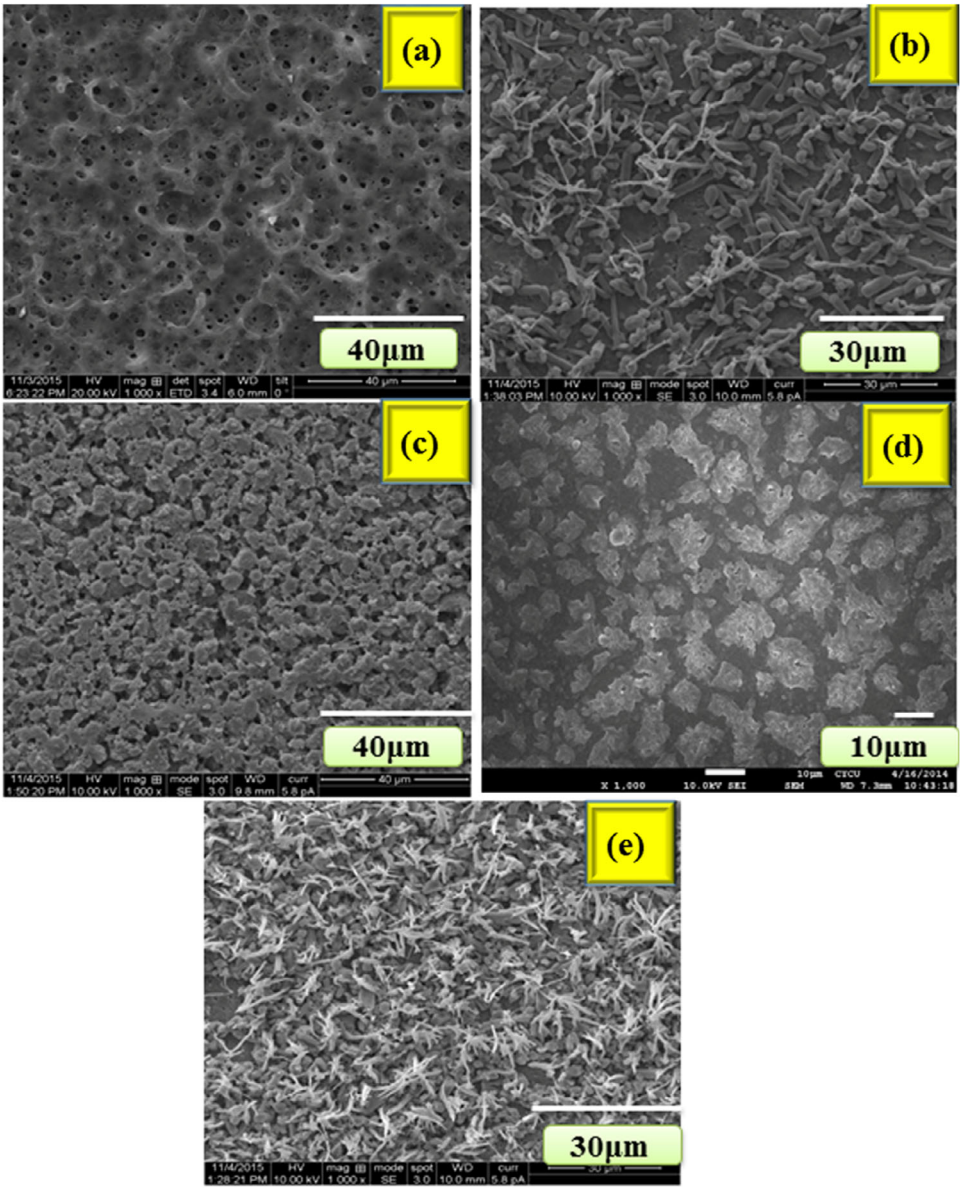

FIGURE 4 SEM images of (a) bare P(S-MMA) –PVdF- $LiClO_4$-EC + PC (b) 3 (c) 6 (d) 9 (e) 12 wt% of ZrO_2 based P(S-MMA)-PVdF-$LiClO_4$– based polymer electrolyte [Color figure can be viewed at wileyonlinelibrary.com]

electrolyte - ZrO_2 (6) wt%. The sample shows a weight loss of about 3–10% at 100°C, it may be due to the presence of wetness, while loading the sample for the analysis. The second decomposition of the sample happens around 320°C, it may due to the expelling of the plasticizers. Beyond which the film is found to lose its weight drastically causing the disintegration of the electrolyte matrices. This decomposition is endorsed to the copolymer breaking bonds (C—H, C—F) in the polymer matrices. Nearly 6% of the residues have been observed for samples which may be due to the presence of inorganic filler ZrO_2 in the complexes. It is obvious from the observation that the film containing 6 wt% of ZrO_2 combination exhibited higher conductivity of ions and thermal steadiness up to 270°C. The DTA curves of all samples entrust the decomposition of the polymeric materials as analyzed in the thermogravimetric curve.

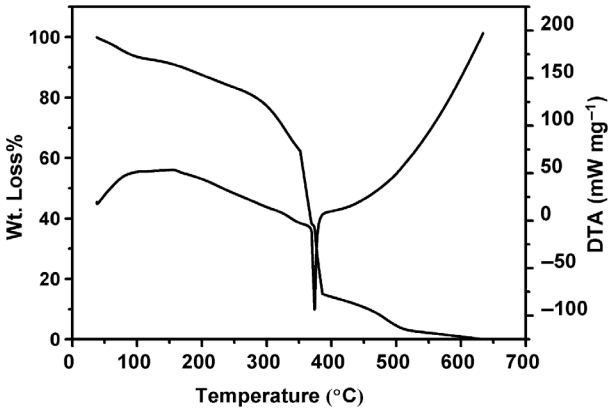

FIGURE 5 TG/DTA (DTA stands for differential thermal analysis) curves of P(S-MMA)-PVdF(25:75 of 27 wt%)-$LiClO_4$(8 wt %)-EC:PC (1:1 of 65 wt%)- ZrO_2 (6) wt% based polymer electrolyte

3.6 | Linear sweep voltammetry and cyclic voltammetry analyses

Figure 6(a) depicts the linear sweep voltammetry curve of SS/ ZB3/Li cell. It can be seen from Figure 6(a), as voltage increases through the electrolyte ZB3, no current flows through the electrolyte up to 4.5 V, beyond which the electrolyte allows the current to pass through it rapidly, which reveals the electrolyte's decomposition. This disintegration of the electrolyte is observed around 4.6 V, indicates the oxidative steadiness of the matrices. This is a significant parameter for the application of electrolytes in high voltage battery fabrication. The electrochemical performance of the as-synthesized composite gel electrolyte matrices has been evaluated using (CR 2032 type coin cell) $LiFePO_4$/ZB3/Li half-cell at 0.5 mV s^{-1}. The cyclic voltammetry of the cell is performed over a voltage array between 2 and 4.3 V versus Li^+ at scan proportion of 1 mV s^{-1} at 303 K, which has been depicted in Figure 6(b). The oxidation and reduction peaks have appeared at a potential of 3.33 and 3.05 V respectively. A similar trend was observed from the literature.[37,41,42]

3.7 | Charge/discharge profile analyses

Figure 7 shows a typical charge–discharge profile of the fabricated ZB3 electrolyte-based sample at 0.1 C rate under room temperature with cut-off voltage 2 to 4.3 V, the initial charge and discharge capacities are 162 and 144 mAh g^{-1} with the coulombic efficiency of 88.8%. The prepared sample attained 84.7% of the theoretical value, representing that the $LiFePO_4$ created in that work has good kinetics and that it can efficiently function in a battery having a polymer electrolyte. The stable potential range in the charge/discharge profile shows good electrochemical stability. In the fifth cycle, the cell brings a

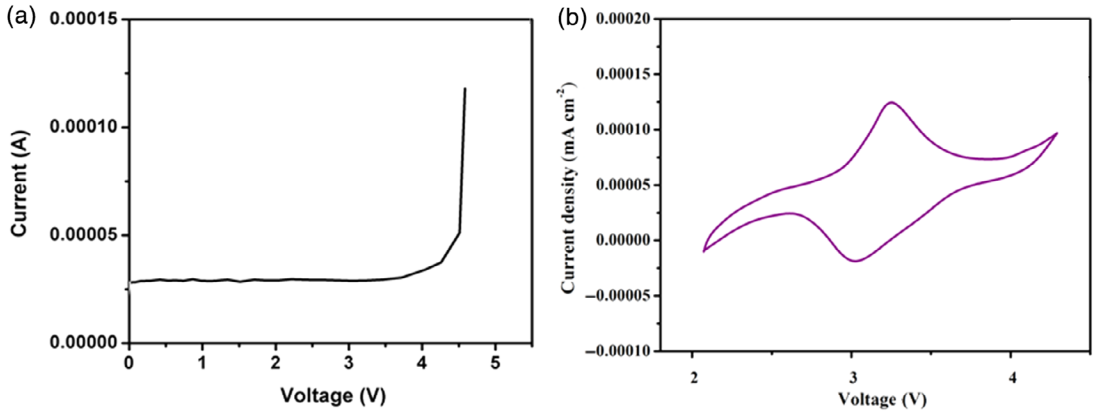

FIGURE 6 (a) Linear sweep (b) cyclic voltammogram of $LiFePO_4$/ P(S-MMA)-PVdF-$LiClO_4$-EC + PC–6 wt% ZrO_2 (ZB3)/Li cell [Color figure can be viewed at wileyonlinelibrary.com]

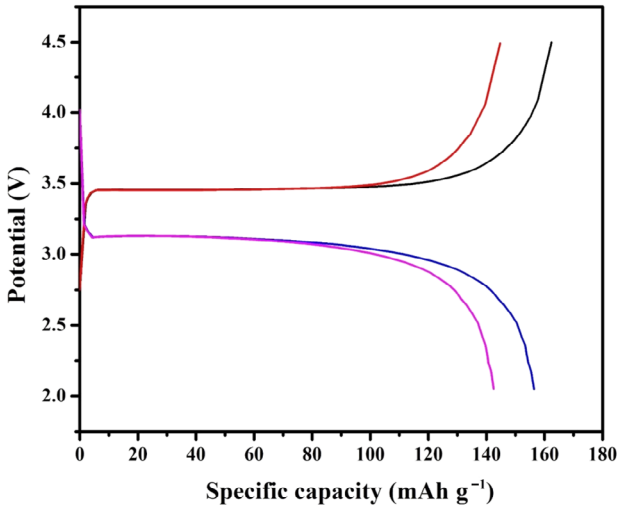

FIGURE 7 Initial chare/discharge profile of $LiFePO_4$/ P(S-MMA)-PVdF-$LiClO_4$-EC + PC–6 wt% ZrO_2 (ZB3)/Li cell [Color figure can be viewed at wileyonlinelibrary.com]

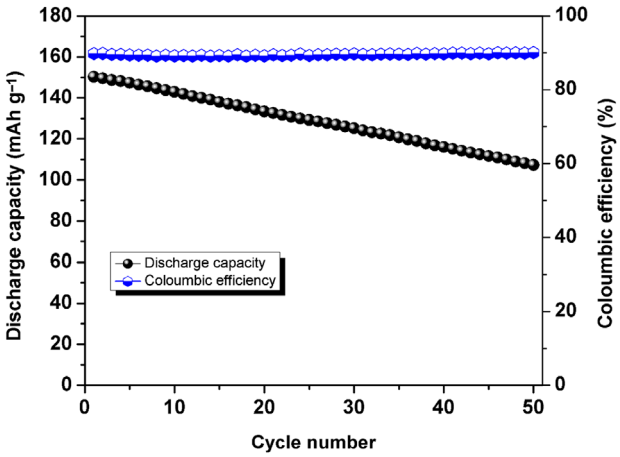

FIGURE 8 Cyclic stability of $LiFePO_4$/ ZB3/ Li cell at 0.1 C rate between 2 to 4.3 V [Color figure can be viewed at wileyonlinelibrary.com]

reversible capacity of 142 mAh g^{-1} with a capacity retention of 98.6% has been attained. These results confirm the prepared polymer electrolyte effectively enhances the performance of the lithium-ion battery.

Figure 8 illustrats the performance Li/CPE/$LiFePO_4$ cell at 0.1 C rate. The composite gel electrolyte displays auspicious characteristics such as capacity retention and coulombic efficiency. Upon continuous cycling, the coulomic efficiency of the electrolyte is 88.8%. The discharge capacity is observed from initial and 50th cycle is 144 and 107 mAh g^{-1} respectively at 0.1 C rate with capacity retention is 74.3%. The observed values are correlated with the cyclic behavior of batteries Li/$LiFePO_4$ with composite polymer electrolyte.[39,43] Hence, the better electro chemical performance of CPE is due to the inclusion of ZrO_2 in the electrolyte.

4 | CONCLUSION

The ZrO_2 filler (bare, 3, 6, 9, and 12) wt% had been dispersed into the prepared P(S-MMA)-PVdF-$LiClO_4$-EC + PC complex. The as-prepared films had been subjected to study structural, functional, thermal, morphology, impedance, and luminescence properties. The amorphous structures, complexation behavior of the synthesized films was established through X-ray diffraction and FT-IR technique respectively. Thermal stability of the polymer electrolyte was up to the temperature 270°C is ascertained through TG analysis. The enhanced ionic conductivity by adding the PVdF with the parent electrolyte was 1.2×10^{-2} S cm^{-1} at 303 K for the 6 wt% ZrO_2 based system. This linear increase in conductivity was due to the role of plasticizer mixture and the blend polymer PVdF which had also possessed a higher dielectric constant that is, 8.4. The decomposition of the electrolyte is observed around 4.6 V, using LSV studies, indicates the oxidative stability of the electrolyte. The oxidation and reduction peaks had appeared at a potential of 3.33 and 3.05 V respectively using cyclic voltammetry studies. The charge/ discharge profile of the half cell is performed for 50 cycles to confirm the stability of the battery using battery tester at 0.1 C rate. The discharge capacity of 144 mAh g^{-1} with the 88.8% coulomic efficiency and with capacity retention of 74.3%. The optimized nanocomposite polymer electrolyte system has been used as the probable device manufacture in the rechargeable lithium batteries.

ACKNOWLEDGMENTS

M. S. gratefully acknowledges for UGC-New Delhi financial support under UGC-MRP F.NO. 41-839/2012. All authors from Alagappa University acknowledge the financial support by DST-SERB, New Delhi, under the Physical Sciences grant sanctioned vide EMR/2016/006302. Also, all the authors gratefully acknowledge for extending the analytical facilities in the Department of Physics, Alagappa University under the PURSE program, sponsored by the Department of Science and Technology (DST), New Delhi, Government of India, and Ministry of Human Resource Development RUSA-Phase 2.0 grant sanctioned vide Lt.No. F-24-51/2014 U Policy (TNMulti Gen), Department of Education, Government of India.

ORCID

Marimuthu Sivakumar https://orcid.org/0000-0002-7138-8220

REFERENCES

[1] O. Padmaraj, M. Venkateswarlu, N. Satyanarayana, *RSC Adv* **2016**, *6*, 6486.
[2] J. R. Nair, M. Destro, F. Bella, G. B. Appetecchi, C. Gerbaldi, *J. Power Sources* **2016**, *30*, 258.
[3] T. Dam, S. N. Tripathy, M. Paluch, S. S. Jena, D. K. Pradhan, *Electrochim. Acta* **2016**, *202*, 147.
[4] A. Subramania, N. T. Kalyanasundaram, A. R. Sathiyapriya, G. Vijayakumar, *J. Membr. Sci.* **2007**, *294*, 8.
[5] F. Croce, G. B. Appetecchi, L. Persi, B. Scrosati, *Nature* **1998**, *394*, 456.
[6] J. M. Tarascon, M. Armand, *Nature* **2001**, *414*, 359.
[7] K. Murata, S. Izuchi, Y. Yoshihisa, *Electrochim. Acta* **2000**, *45*, 1501.
[8] N. Angulakshmi, S. Thomas, K. S. Nahm, A. M. Stephan, R. N. Elizabeth, *Ionics* **2011**, *17*, 407.
[9] M. A. Brza, S. B. Aziz, H. Anuara, F. Ali, *Polym. Test.* **2020**, *91*, 106813.
[10] K. Ariga, J. Li, *Adv. Mater* **2016**, *29*, 978.
[11] K. Kimara, H. Matsumoto, J. Hagsoun, S. Panero, B. Scorsati, *Electrochim.Acta.* **2015**, *175*, 134.
[12] K. Jeddi, K. Sarikhani, N. T. Qazvini, P. Chen, *J. Power Sources* **2014**, *245*, 656.
[13] Y. Ma, L. B. Li, G. X. Gao, X. Y. Yang, You, *Electrochim. Acta* **2016**, *187*, 535.
[14] S. Austinsuthanthiraraj, R. Kumar, B. Josephpaul, V. Mathew, *Solid State Electrochem* **2011**, *15*, 561.
[15] P. Vickraman, D. Ravindran, *Ionics* **2011**, *17*, 565.
[16] M. Ramachandran, R. Subadevi, W.-R. Liu, M. Sivakumar, *J. Nano.Sci.Nano.Tech.* **2018**, *18*, 368.
[17] S. Rajendran, T. Uma, *Ionics* **2001**, *7*, 122.
[18] F. Capuano, F. Croce, B. Scrosati, *Electrochem. Soc* **1991**, *138*, 1918.
[19] S. Rajendran, O. Mahendran, T. Mahalingam, *Eur. Polym. J.* **2002**, *38*, 49.
[20] T. Pareek, S. Dwivedi, S. A. Ahmad, M. Badole, S. Kumar, *J. Alloys Compds* **2020**, *824*, 153991.
[21] K. Chen, D. Xue, Q. D. Su, *Colloid Interface Sci.* **2015**, *446*, 77.
[22] Q. Wang, C. Li, M. Guo, C. Hu, Y. Xie, *J. Mater. Chem. A* **2014**, *2*, 1346.
[23] F. Ahmed, S. Kumar, N. Arshi, M. S. Anwar, L. S. Yeon, G. Sukkil, D. W. Park, B. H. Koo, C. G. Lee, *Thin Solid Films* **2011**, *519*, 8375.
[24] C. V. S. Reddy, Q. Y. Zhu, L. Q. Mai, W. J. Chen, *Solid State Electrochem.* **2007**, *11*, 543.
[25] S. Rajendran, M. Sivakumar, R. Subadevi, *J. Appl. Polym. Sci.* **2003**, *90*, 2794.
[26] M. Hema, P. Tamilselvi, *J. Phy. Chem. Solids.* **2016**, *96-97*, 42.
[27] M. Sivakumar, R. Muruganantham, R. Subadevi, *RSC Adv.* **2015**, *5*, 86126.
[28] Y. Liu, J. Y. Lee, L. Hong, *Solid State Ionics* **2002**, *150*, 317.
[29] Z. He, Q. Cao, B. Jing, X. Wang, Y. Deng, *RSC Adv.* **2017**, *7*, 3240.
[30] A. M. Stephan, *Eur. Polym. J.* **2006**, *42*, 21.
[31] A. M. Stephan, S. G. Kumar, N. G. Renganathan, M. A. Kulandainathan, *Euro. Poly. J.* **2005**, *41*, 15.
[32] F. Croce, L. Persi, B. Scrosati, F. Serraino-Fiory, E. Plichta, M. A. Hendrickson, *Electrochim. Acta* **2001**, *46*, 2457.
[33] X. Qian, N. Gu, Z. Cheng, X. Yang, E. Wang, Dong, *Electrochim. Acta* **2001**, *46*, 1829.
[34] M. Sivakumar, R. Subadevi, S. Rajendran, H.-C. Wu, N.-L. Wu, *Euro. Poly. J.* **2007**, *43*, 4466.
[35] M. A. AL-Akhras, S. E. Alzoubi, A. A. Ahmad, R. Ababneh, A. Telfah, *J. Appl. Poly. Sci.* **2021**, *138*, 49757.
[36] T. Miyamoto, K. Shibayama, *J. Appl. Phys.* **1973**, *44*, 5372.
[37] S. Suriyakumar, M. Raja, N. Angulakshmi, K. S. Nahmb, A. M. Stephan, *RSC Adv.* **2016**, *6*, 92020.
[38] J. Hu, P. He, B. Zhang, B. Wang, L. Z. Fan, *Energy Storage Mater.* **2020**, *26*, 283.
[39] X. Pan, F. Lian, Y. He, Y. Peng, X. Sun, Y. Wen, H. Guan, *J. Appl. Poly. Sci.* **2015**, *132*, 41839.
[40] V. Aravindan, P. Vickraman, *Ionics* **2007**, *13*, 277.
[41] A. Guerfi, S. Duchesne, Y. Kobayashi, A. V. K. Zaghi, *J. Power Sources* **2008**, *175*, 866.
[42] Y. Zhang, C. Y. Wang, X. Tang, *J. Power Sources* **2011**, *196*, 1513.
[43] S. Ferrari, E. Quartarone, P. Mustarelli, A. Magistris, M. Fagnoni, S. Protti, C. Gerbaldi, A. Spinella, *J. Power Sources* **2010**, *195*, 559.

SUPPORTING INFORMATION

Additional supporting information may be found online in the Supporting Information section at the end of this article.

How to cite this article: M. Ramachandran, R. Subadevi, P. Rajkumar, R. Muthupradeepa, M. Sivakumar, *J Appl Polym Sci* **2021**, e51180. https://doi.org/10.1002/app.51180